Communicated by William Lytton

Effects of Input Synchrony on the Firing Rate of a Three-Conductance Cortical Neuron Model

Venkatesh N. Murthy*
Eberhard E. Fetz
Department of Physiology and Biophysics and Regional Primate Research Center, University of Washington, Seattle, WA 98195 USA

For a model cortical neuron with three active conductances, we studied the dependence of the firing rate on the degree of synchrony in its synaptic inputs. The effect of synchrony was determined as a function of three parameters: number of inputs, average input frequency, and the synaptic strength (maximal unitary conductance change). Synchrony alone could increase the cell's firing rate when the product of these three parameters was below a critical value. But for higher values of the three parameters, synchrony could reduce firing rate. Instantaneous responses to time-varying input firing rates were close to predictions from steady-state responses when input synchrony was high, but fell below steady-state responses when input synchrony was low. Effectiveness of synaptic transmission, measured by the peak area of cross-correlations between input and output spikes, increased with increasing synchrony.

1 Introduction

Synchronous activity in the millisecond time range has been observed in many regions of the brain. Cross-correlation histograms between spike trains from neocortex of mammals often exhibit central peaks on this time-scale (Fetz *et al.* 1991; Nelson *et al.* 1992). The possible function of synchronous neural activity in the mammalian brain has attracted renewed interest in light of recent reports that many neurons are synchronously coactivated in the visual cortex (Eckhorn *et al.* 1988; Gray and Singer 1989; Engel *et al.* 1991) and sensorimotor cortex (Bouyer *et al.* 1981; Murthy and Fetz 1992; Llinás and Ribary 1993; Sanes and Donoghue 1993).

While synchronous activity could simply reflect the consequences of convergent neural circuitry, it could also play a significant role in neural transmission. The present study explores the role of synchrony in determining firing rates of a model neuron. Postsynaptic potentials have finite

*Current address: The Salk Institute, CNL, 10010 N. Torrey Pines Road, La Jolla, CA 92037 USA.

time constants and their amplitudes are usually a small fraction of the depolarization necessary to evoke a spike. Therefore, near-simultaneous arrival of spikes is likely to be more effective in depolarizing a cell to threshold than asynchronous inputs, especially when the interspike intervals are greater than the membrane time constant. Relatively few studies have investigated this issue parametrically (Abeles 1982, 1991; Kenyon *et al.* 1990; Reyes and Fetz 1993; Murthy and Fetz 1993; Bernander *et al.* 1994).

A primary aim of our simulations was to describe quantitatively how the output of a biophysically based model neuron depends on the degree of synchrony in its inputs. Further, we wanted to determine the parameter regime in which synchrony could play a significant role. We systematically explored the effect of the following parameters on the average output firing rate (f_o): (1) N, the number of inputs to the model neuron, (2) f_i, the average firing rate of each input, (3) w, the synaptic efficacy defined as the maximal unitary synaptic conductance, and (4) s, the degree of synchrony among the inputs (varied from 0 to 100%). We found that for low values of the first three parameters, synchrony increased f_o, whereas for higher values of these parameters, synchrony could in fact reduce f_o. Preliminary results were presented at the Computation and Neural Systems 1992 meeting (Murthy and Fetz 1993).

2 Methods

The driven neuron was modeled to represent a cortical pyramidal cell. It had five compartments: a soma and four apical dendritic compartments (Fig. 1a). We chose a simplified biophysical model because it has been shown to reproduce many of the features of more detailed compartmental models (Lytton and Sejnowski 1991; Bush and Sejnowski 1993). Three Hodgkin–Huxley style membrane currents were included in the soma: fast sodium, delayed rectifier potassium, and an A-like potassium current (the A-current was included to generate low-frequency firing in response to injected current). The parameters for the kinetics of the currents were similar to those of the three-channel model of Lytton and Sejnowski (1991), and are listed in Table 1. The dendritic compartments did not have any nonsynaptic active currents. The excitatory synaptic inputs occurred equally on the second and the third dendritic compartments and were modeled with a conductance change whose time course was similar to the fast glutamate synapses in the cortex (Hestrin 1992). The conductance change was modeled as a sum of two exponentials, with a rise time constant of 0.5 msec and a decay time constant of 1 msec:

$$g_{syn}(t) = \bar{g}\left(-e^{-t/0.5} + e^{-t}\right) \tag{2.1}$$

where t is time in milliseconds and $\bar{g}$ is a scaling factor that determined the maximal conductance w in units of Siemens. The strength of the input connections was varied by changing $\bar{g}$. For each w, the peak of the EPSP

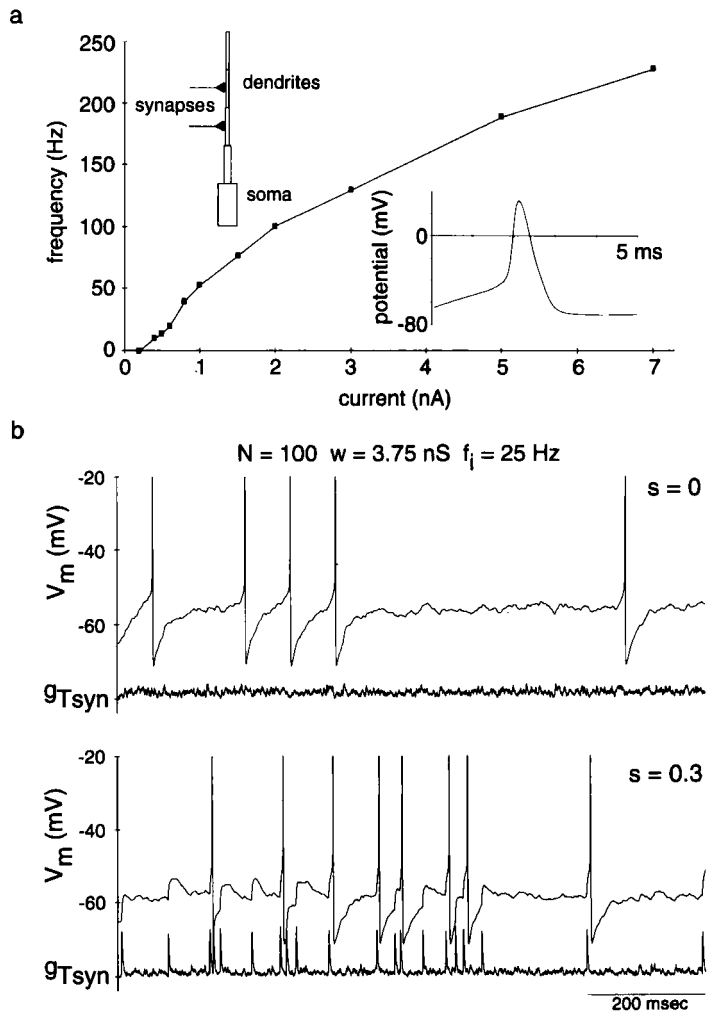

Figure 1: Responses of the model cell. (a) Steady-state firing rate vs. injected current determined by injecting 500 msec current steps into the soma. Insets show schematic of the model cell and an action potential evoked by injecting 0.5 nA current for 1.5 msec. (b) The membrane potential (V_m) in the soma compartment and the total synaptic conductance ($g_{T_{syn}}$) at the second dendritic compartment for two levels of synchrony in the inputs. For both panels, N = 100, f_i = 25 Hz, w = 3.75 nS (200 μV). In the bottom panel (s = 0.3) the large transients in the membrane potential directly cause spikes. Action potentials are truncated.

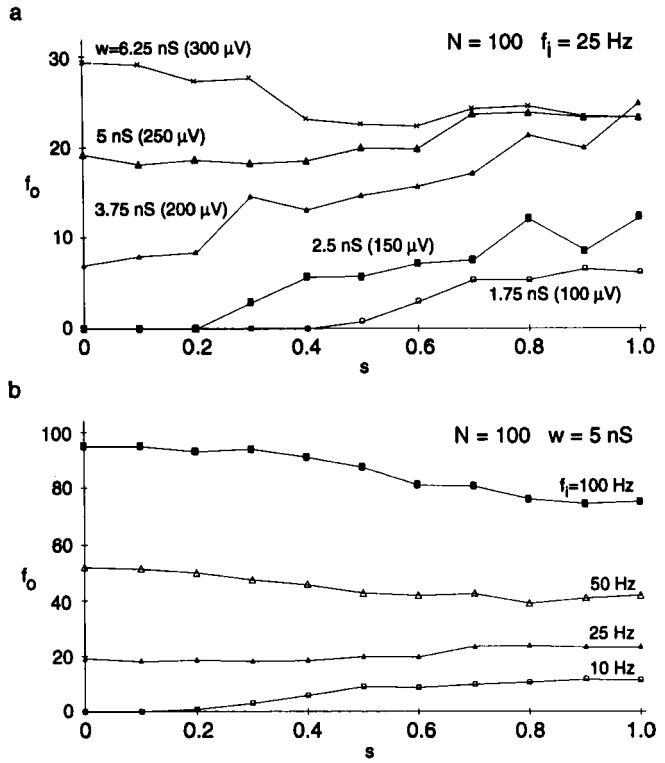

Figure 2: (a) Dependence of f_o on synchrony and synaptic strength w, for $N = 100$, $f_i = 25$ Hz. Each curve represents the relation between f_o and s for a particular value of w. The coefficient of variation of f_o (variance divided by mean) increased nearly linearly with synchrony. (b) Dependence of f_o on synchrony and input frequency, for $N = 100$, $w = 5$ nS (250 μV). Each curve represents the relation between f_o and s for a particular value of f_i.

from resting membrane potential was determined, since this is the most common experimentally measured quantity. Corresponding values of w and EPSP amplitudes are given in Figure 2. Inhibitory inputs were not systematically explored in these simulations. The input spike trains were modeled as Poisson processes and all inputs in a given simulation had the same mean rate. The total number of inputs was either 50, 100, or 200. These numbers were chosen so that for EPSP sizes and spontaneous firing rates seen in the cortex, the model neuron's firing rate would be in the physiological range. For example, if the inputs had a mean rate of 10 Hz and produced EPSPs of 200 μV, then about 100 inputs would give

rise to a firing rate of 10 Hz in the postsynaptic cell. This number is intended to represent not the total number of anatomical input connections to a cortical neuron, but the mean number of active inputs. No synaptic input other than that specified by N, nor any other source of background activity was included. Synchronization was simulated by lumping multiple inputs into one, whose strength was increased proportionately. When all inputs were independent of each other, the value for the synchrony factor s was defined as 0. The synchrony among the inputs was varied in steps of 0.1 to a maximum value of 1, for 100% synchrony. For example, at "0.3 synchrony," 30% of the afferents had identical spike trains; the other 70% had independent spike trains. The average number of spikes per second (f_o) was used as the measure of the output. All simulations were performed using the computer program GENESIS running on a Sun 4 workstation (Wilson and Bower 1989).

3 Results

The maximal conductances of the fast sodium, delayed rectifier potassium, and the A channels were adjusted to reproduce action potential waveforms and f–I curves seen in cortical pyramidal neurons (Stafstrom *et al.* 1984). With the cell at rest (−65 mV), the passive membrane time constant was 15 msec and the total input resistance was 40 MΩ. The passive time constant of the model was not systematically varied. However, the effective time constant would vary implicitly as a function of synaptic inputs and the activity of the cell (Bernander *et al.* 1991). Figure 1a shows the responses of the model, whose intrinsic parameters were fixed at values in Table 1.

3.1 Steady-State Activity. For each combination of the four parameters N, f_i, w, and s, 5 sec of activity was simulated and the average firing frequency of the cell over this time was calculated. The values of f_o as a function of s were determined with the other three parameters fixed. For sake of clarity, the results are discussed in three sections; each section describes the effect of increasing synchrony on f_o when one variable was varied systematically, with the other two fixed.

1. *N and f_i held constant, w varied*: Figure 1b shows the membrane potential trajectories and the total synaptic conductance for two levels of input synchrony with the other parameters kept constant [$N = 100$, $f_i = 25$ Hz, and $w = 3.75$ nS (200 μV)]. With minimal synchrony ($s = 0$), the membrane potential fluctuations were relatively small and the cell fired intermittently. When the level of synchrony was raised to 0.3, the membrane potential was strongly influenced by the synchronized input, which produced large EPSPs. The average firing rate was higher for $s = 0.3$ than for $s = 0$.

Figure 2a shows a typical family of curves depicting the dependence of f_o on w and s, for $N = 100$ and $f_i = 25$ Hz. For low values of w, the

Table 1: Parameters of the Model

Passive Parameters

Dimensions	Global variables
Soma: 100×10 μm	$r_a = 0.2$ Ω-m
Apical 1: 50×2 μm	$r_m = 1.5$ Ω-m
Apical 2: 50×1.5 μm	$c_m = 0.01$ F m^{-2}
Apical 3: 50×1.0 μm	
Apical 4: 50×1.0 μm	

Active Parameters

Channel	$\bar{g}$ (S/cm^2)	α_{act}	β_{act}	α_{inact}	β_{inact}
Na	0.4	$\frac{-0.32(V+47)}{e^{(V+47)/-4}-1}$	$\frac{0.26(V+25)}{e^{(V+25)/4}-1}$	$0.128e^{(V+48)/-18}$	$\frac{4}{e^{(V+25)/-5}+1}$
K	0.2	$\frac{-0.32(V+50)}{e^{(V+50)/-5}-1}$	$0.5e^{(V+55)/-40}$		
A	0.002	$\frac{0.2}{e^{(V+35)/-7}}$	$\frac{0.2}{e^{(V+35)/28}}$	$\frac{0.09}{e^{(V+45)/14}}$	$\frac{0.09}{e^{(V+45)/-33}}$

Synapse

$g_{syn}(t) = \bar{g}(-e^{\frac{-t}{0.5}} + -e^{-t})$

w = Maximum$[g_{syn}(t)]$ = 1.25 to 6.25 nS

output increased with increasing synchrony. For instance, for an EPSP of 150 μV, no spike was evoked in the model neuron at $s < 0.3$. At $s = 0.3$, an average of four spikes was evoked per second, and at 100% synchrony ($s = 1$), the average output was 10 Hz. Unitary EPSPs of 250 μV ($w = 5$ nS) evoked an average output frequency of about 20 Hz at all levels of synchrony. With even larger EPSPs, f_o actually decreased with increasing synchrony. This occurred when the synaptic strength was large enough to make f_o greater than f_i at low synchrony. At high synchrony all inputs were effectively lumped into one source, and since each EPSP evoked at most one spike in the model, f_o could not be greater than f_i. The excess depolarizing input beyond the amount required to reach threshold was effectively wasted. f_o was actually less than f_i for the highly synchronized inputs since some of the input spikes arrived during the cell's refractory period (see below).

At low levels of synchrony, the individual synaptic currents summed more smoothly and led to a relatively regular firing rate, which could be greater than f_i. As a simple analogy, injecting 2 nA for 20 msec into the soma with a microelectrode can evoke multiple spikes, while injecting a

20 nA current pulse for 2 msec would evoke only 1 spike, even though the total charge is the same. For most of the parameters considered, the coefficient of variation of f_o (variance/mean) increased with increasing synchrony. When the inputs were highly synchronized, the output spikes were more tightly linked with the inputs and therefore tended to have the same statistics (Poisson) as the inputs. Simulations were performed for other values of N and f_i and the results were qualitatively similar to those in Figure 2a.

2. *N and w held constant, f_i varied*: Figure 2b shows the dependence of f_o on s for different values of f_i [$N = 100$ and $w = 5$ nS (250 μV)]. At low values of f_i, increasing synchrony led to an increase in f_o. For example, for $f_i = 10$ Hz, no spike was evoked until $s = 0.2$. For $s > 0.2$, increasing the synchrony led to a steady increase in f_o. As discussed above, this is because for low values of f_i, the membrane potential of the cell seldom reached threshold if the inputs were independent. Synchronizing the inputs led to more frequent threshold crossings and to a greater f_o. For $f_i = 25$ Hz, f_o was relatively independent of synchrony and for $f_i >$ 40 Hz, f_o decreased with increasing synchrony. This behavior is due to the cumulative effect of the refractory period. If the refractory period after each spike is r, then the total amount of refractory time per second is rf_o, where r represents the entire postspike period during which the fully synchronized input is incapable of producing a spike (r depends on w in addition to intrinsic parameters of the cell). When input spikes are fully synchronized ($s = 1$) and are sufficient to evoke a postsynaptic spike from resting level, the output firing rate at $s = 1$ (denoted as f_o^1) is given by

$$f_o^1 = f_i(1 - rf_o^1) \tag{3.1}$$

Therefore,

$$f_o^1 = \frac{f_i}{1 + rf_i} \tag{3.2}$$

At low values of f_i, $rf_i \ll 1$ and f_o^1 is almost equal to f_i. As f_i increases, the rf_i term causes f_o^1 to become significantly less than f_i (Fig. 3). At the other extreme of zero synchrony the output frequency (f_o^0) can be determined by the steady state f–I curve (Fig. 1a), with the injected current approximated by the sum of all the asynchronous synaptic inputs. For the parameters considered in Figure 2b, the f_o^0 and f_o^1 curves crossed at $f_i \approx 40$ Hz (Fig. 3). Above that value of f_i, f_o decreased with increasing s. Although this crossover point was different for other values of N and w, qualitatively similar results were obtained.

3. *w and f_i held constant, N varied*: Changing N was essentially equivalent to changing f_i, because each of the inputs had the same mean rate and statistics, and the sum of Poisson processes is another Poisson process. However, by keeping the number of inputs and the mean rate of each distinct, synchrony could be interpreted physically by assigning one

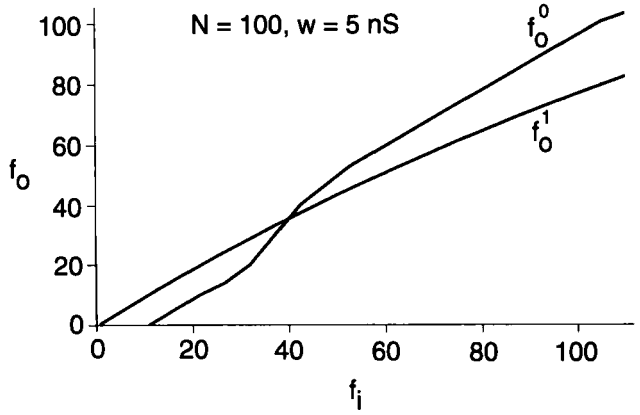

Figure 3: Dependence of f_o on f_i at two extremes of input synchrony, for $N = 100$, $w = 5$ nS (250 μV). f_o^1 is the curve for $s = 1$, as calculated using equation 3.2 with $r = 3$ msec (this is the refractory period for the specific N and w used). f_o^0 plots output frequency for $s = 0$, as estimated from the f–I curve in Figure 1a assuming that the total injected current was

$$Nf_i\overline{V_m}\int_0^\infty g_{syn}(t)\,dt$$

$\overline{V_m}$ is the average potential difference driving the synaptic currents and $g_{syn}(t)$ is the unitary synaptic conductance change (equation 2.1). The two curves cross over at $f_i \approx 40$.

presynaptic neuron to each input. For this reason, N and f_i were treated explicitly as two separate parameters. In the parameter range we have considered, increasing N had an effect similar to that of increasing f_i. That is, for a given w and f_i, for low values of N, f_o increased with s, and above a certain value of N, f_o decreased with s.

It is of interest to determine how the three factors N, w, and f_i can be combined to predict when the synchrony among inputs would increase the firing rate of the cell. Synchrony was considered to have a significant effect on f_o, if f_o increased by at least 10% when synchrony was changed from 0 to 1. With this criterion, synchrony was found to have a significant effect on f_o if the product of the three factors N, w, and f_i, denoted by P, was less than 9.4 μS sec^{-1}. That is,

$$P = Nwf_i < 9.4\ \mu S\ \text{sec}^{-1} \tag{3.3}$$

If w is expressed as EPSP amplitude, this value would correspond to 0.5 Vsec^{-1} (assuming a linear relation between the conductance and the

resultant EPSP at rest). This particular cut-off for P depends on the choice of model cell and parameters. For instance, if the resting membrane time constant is halved, synchrony will be effective for P up to 18.8 μS sec^{-1}.

3.2 Time-Varying Inputs. The above results pertain to measures of average steady-state firing rates of the neuron. To determine whether these results would also hold for changing rates, we measured responses to step and sinusoidal variations in input rates.

1. *Step changes in* f_i: For a particular value of N, w, and s, a step increase in f_i from 25 to 50 Hz was introduced at $t = 0$ sec. A histogram was constructed from the spike trains showing the firing rates before and after this change, as illustrated in Figure 4a. At $t = 0$ sec the firing rate increased to a new level within 15 msec for $s = 0.4$, comparable to the time constant of the membrane. This transient phase was shorter for $s = 0.8$ because the synchronous inputs dominated the response and caused the increase in firing rate to occur faster than the membrane time constant. Similar results were obtained for other step changes in rate. In addition to the transient due to the membrane time constant, a phasic component in the response would be expected to occur if the model had included membrane currents that cause adaptation of firing frequency. For parameter values in the ranges considered in the previous section, the output frequencies were predicted well by the values of f_o obtained from the steady-state simulations.

2. *Sinusoidal variation of* f_i: The input firing rate was modulated sinusoidally about a mean value $\bar{f}_i$, as determined by the formula

$$f_i(t) = \bar{f}_i[1 + \delta \sin(2\pi\nu t)] \tag{3.4}$$

The modulation frequency ν was arbitrarily set to 10 Hz and δ, the depth of modulation about the mean, was set to 0.5. For a simulation of 40-sec duration, a cycle-triggered time histogram was compiled by aligning the responses on a specific phase. Figure 4b shows one such compilation for two values of synchrony, $s = 0$ and $s = 0.5$. For low synchrony, the output was a distorted sinusoid, with sharp responses at the peaks and cut-off in the troughs. The distortion was produced by modulation around threshold and the low-pass characteristics of the membrane, which led to a slow depolarization during the positive phase of the input sinusoid, producing output spikes near the peak. Moderate synchrony in the inputs produced more jitter in the spike times, making the f_o sinusoids smoother. The response to sinusoidal modulations of input frequency was close to that predicted by steady-state curves such as those in Figure 2a for values of $s \geq 0.3$ (Fig. 4b, bottom). For $s < 0.3$, the sinusoidal inputs led to a greater peak f_o than predicted by the steady state and a smaller f_o at the troughs (Fig. 4b, top). This occurred because the synaptic currents during the troughs of the input sinusoids were insufficient to evoke spikes by themselves but helped to slowly depolarize the cell. In effect, the spiking near the peaks of the sinusoids included contributions

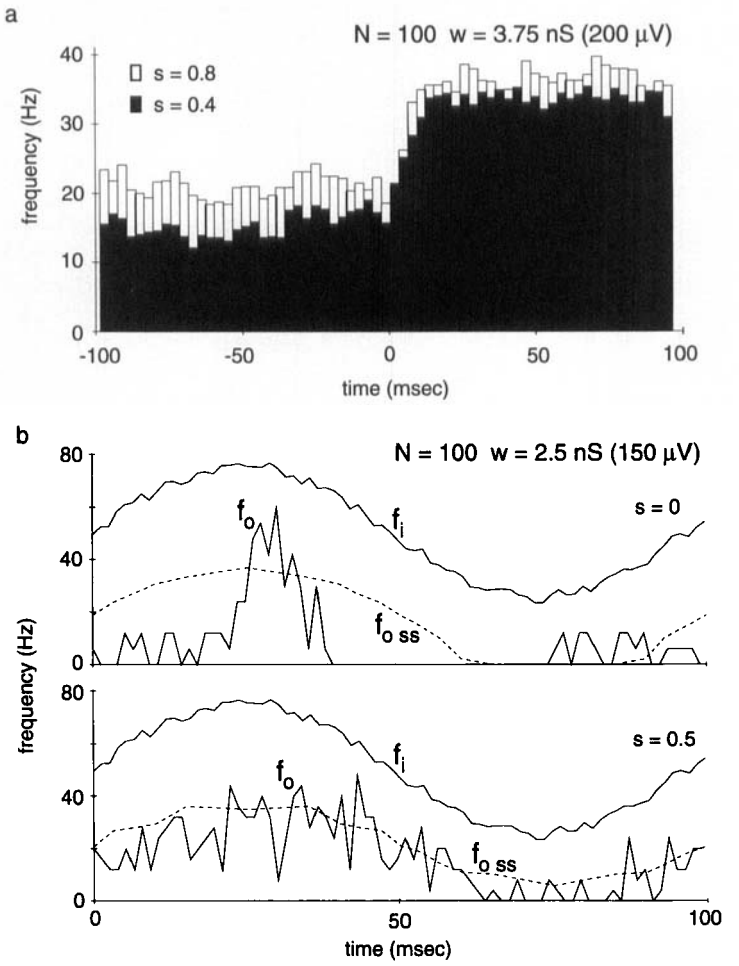

Figure 4: Effect of synchrony on responses to modulated inputs. (a) Histograms of f_o when the input frequency was stepped from 25 to 50 Hz at $t = 0$ sec. $N = 100$, $w = 3.75$ nS (200 μV), and s was 0.4 (black bars) or 0.8 (light bars). The binwidth was 3 msec. (b) Histograms of spikes from sinusoidally modulated inputs (f_i), from the model cell (f_o) and the predicted steady-state response ($f_{o_{ss}}$), for two values of s. $N = 100$, $w = 2.5$ nS (150 μV), and f_i was varied sinusoidally about a mean frequency of 50 Hz. With all independent inputs ($s = 0$), the spikes were clustered near the peak of the input frequency (top). When $s = 0.5$, the spikes were distributed more evenly and were predicted well by steady-state rates.

of synaptic currents from the troughs. Therefore, the f_o obtained from steady-state curves underestimated the firing rates at the peaks of the sinusoids.

3.3 Cross-Correlations. The results above show that for certain parameters, synchrony does not alter the output firing rate. For those parameters we examined, the cross-correlation histogram (CCH) between the synchronous input and the output spikes; the CCH peak area measures the probability of evoking a postsynaptic spike in association with the input spikes. Figure 5 shows a simulation in which $N = 100$, $f_i = 50$ Hz, $w = 2.5$ nS (150 μV), and the levels of synchrony were 0.1, 0.3, 0.5, 0.7, and 0.9. Figure 5a shows the CCH for three levels of synchrony in the input (aligned on the spikes in synchronous units). For these parameters, the average firing rate of the postsynaptic cell did not change with increasing synchrony, as seen by the similar baselines in the histograms. However, increasing synchrony produced an increase in the CCH peak. The cumulative sum (cusum) of the CCH was calculated as the integral of the CCH values minus the average pre-trigger counts (to the left of the origin). The resultant cusum levels show that the probability of evoking a postsynaptic spike for every synchronized input spike increased with increasing input synchrony (Fig. 5b). However, the probability normalized to the number of inputs that were synchronized (the area under the CCH peak/sN) was actually smaller for higher values of s, because the excess depolarization above that required to fire the cell increased with synchrony. Therefore, the effective contribution of an individual synchronized input decreased as other synchronized inputs were added.

4 Discussion

A major objective of this study was to determine parametrically the conditions under which synchrony in the inputs affected the average output firing rate of a biophysical model of a cortical neuron. An interesting finding was that increased synchrony could decrease as well as increase average firing rate. For small values of input firing rates, number of inputs and EPSP amplitude, synchrony could play an important role in increasing the output firing rate. In this parameter range, the membrane potential trajectory was relatively smooth for asynchronous inputs, whereas synchronized inputs caused large deviations in the membrane potential, which often led to spikes (Fig. 1b). The size of unitary EPSPs in cortical pyramidal neurons is in the range of a few hundred microvolts (Thomson *et al.* 1988; Fetz *et al.* 1991; Mason *et al.* 1991; Chen and Fetz 1993). Using a value of 3.75 nS (200 μV) for w, equation 3.3 predicts that synchrony will increase the firing rate when the total rate at which input spikes arrive is less than 2500 sec^{-1}. When N, f_i, and w were large, asynchronous inputs could produce output rates higher than the firing rates

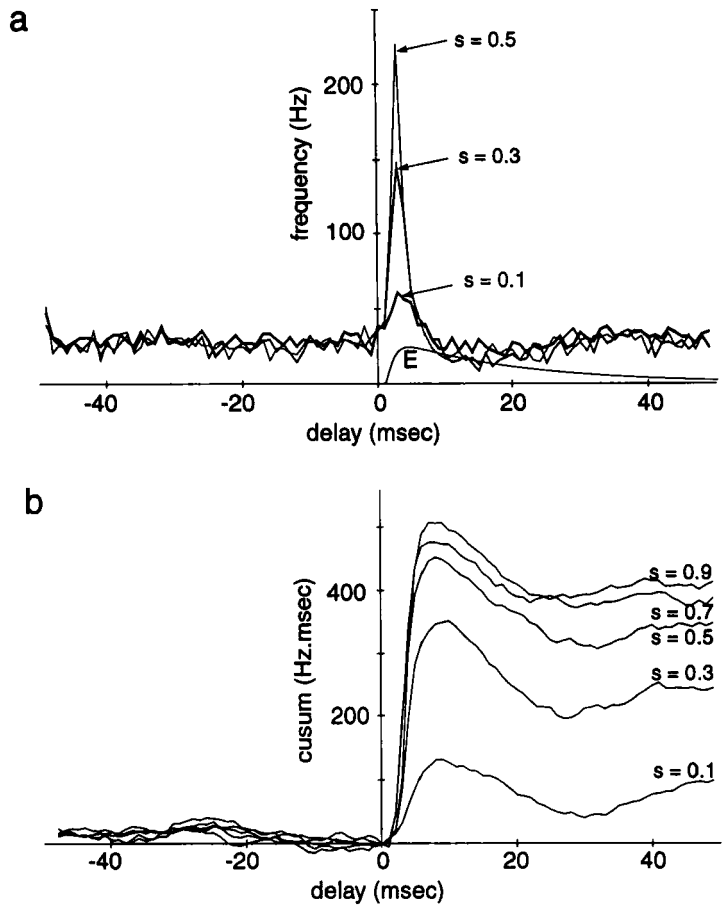

Figure 5: (a) Cross-correlation between the synchronized spikes and the output spikes at three levels of synchrony [$N = 100$, $w = 2.5$ nS (150 μV), $f_i = 50$ Hz]. The background frequency of the model cell was around 30 Hz for all three cases. The EPSP (E) is shown on the same time-scale for comparison. (b) The cumulative sum of the correlograms for five levels of synchrony indicated at the right-hand side of each line. The small rise in the cusum at around −30 ms is due to the rhythmic firing of the post-synaptic cell.

of the individual inputs. In contrast, highly synchronized inputs caused at most one spike for each large synchronized EPSP. Therefore, although there is an efficient one-to-one transfer of spiking, f_o could not exceed f_i. So, in this parameter regime (large Nwf_i), synchrony could actually

reduce f_o. In agreement with our findings, Bernander *et al.* (1994) have recently shown that the number of output spikes evoked by a fixed number of inputs to an integrate-and-fire model increases with synchrony up to a point, after which further synchrony reduces the number of output spikes. They primarily measured the effectiveness of a fixed number of inputs in activating the postsynaptic cell from rest as a function of temporal dispersion of the inputs. For repetitive inputs to an integrate-and-fire model, they determined analytically the parameter space in which synchrony could increase output firing rate. Their equation for the boundary between the parameter domains in which synchrony increased and decreased output firing rates (equation 5 in Bernander *et al.* 1994) can be approximated by the equation $Nwf_i = 0.6$ V sec^{-1} for $f_i < 100$ (using $\tau_m = 17$ msec, threshold = 10 mV above resting membrane potential), which is close to our equation 3.3. The fact that the behavior of our biophysical model is in close quantitative agreement with calculations from their integrate-and-fire model further strengthens the overall conclusions.

The range of parameters in which synchrony could increase firing rates would be altered if the model neuron were made more complex in various ways: (1) Multiple spikes per EPSP could be produced by active membrane currents such as the persistent sodium current, calcium currents that cause bursts of spikes, and long NMDA currents in the postsynaptic response. (2) If membrane currents that exhibit strong inactivation (known to be present in cortical neurons) are included in the model, the neuron will be more sensitive to transient depolarizations such as those arising from synchronous inputs, than to steady depolarization. It has been demonstrated experimentally that EPSPs and transient current pulses injected into cat neocortical neurons *in vitro* increase firing rates more effectively than similar net currents injected steadily (Reyes and Fetz 1993). (3) If inputs are distributed over the dendrites, synchronized inputs can occur on different parts of the dendritic tree, resulting in less cancellation. Further, dendrites with active currents can alter the effective time constant locally and make the neuron more sensitive to specific patterns of inputs (Softky and Koch 1992). Further simulations using models that include these features would be necessary to address these issues.

The results from our simulations of the steady-state condition were compared to the instantaneous response to modulated inputs. For step changes in input frequency and sinusoidally modulated input frequency, the membrane time constant dominated the transient response under conditions of low input synchrony. The cell behaved as an integrator of synaptic inputs for low input synchrony, and produced spikes when threshold was reached. For highly synchronized inputs, the cell produced spikes predominantly in response to synchronized inputs and the time taken for the membrane potential to reach threshold became much smaller. Thus synchrony overcame the slow transient due to the mem-

brane time constant, therefore mitigating the low-pass behavior of the neuron.

Instead of using f_o, the effect of synchrony could also be assessed by the probability of evoking a spike in the output cell for each input spike; the net probability increased with increasing synchrony. In our simulations this was observed as an increase in the peak of the cross-correlation between synchronous input and the output spike trains. However, the probability of evoking an output spike normalized to the number of inputs that were synchronized decreased with increasing synchrony. Nevertheless, the reliability of evoking a spike within a short interval following a particular event (such as the occurrence of synchronous input spikes) could be important for information coding and transmission, and increasing input synchrony would clearly assure this. Such temporal precision in spiking could also be important for evoking synchronous firing in target neurons. Kenyon *et al.* (1990) showed that when a rate-modulated signal is propagated across many layers of leaky integrate-and-fire neurons, adding a degree of synchrony in the inputs increases the fidelity of transmission of the signal when the firing rates are low. They also found that if the inputs to the first layer had low degrees of synchrony, successive layers had diminishing synchrony as measured by the autocorrelation of spikes pooled from all neurons in the layer. However, for input synchrony $\geq 30\%$, the synchrony between cells of a layer was enhanced in successive layers. Abeles (1982, 1991) also studied synchronous transmission in networks as a function of various parameters and found that for low values of unitary EPSPs and input frequencies, transmission of activity through networks was more effective when neurons within layers were synchronized.

The existence of synchronous activity in the cortex has been documented extensively (Eckhorn *et al.* 1988; Gray and Singer 1989; Fetz *et al.* 1991; Murthy and Fetz 1992; Nelson *et al.* 1992). In addition to extracellular recording studies, intracellular recordings of cortical cells show that the membrane potentials exhibit large fluctuations which are synchronized with waves in local field potentials (Jagadeesh *et al.* 1992; Chen and Fetz 1993). Is this synchronous activity likely to be useful in increasing firing rates in cortical neurons, as compared to asynchronous activity with similar mean rates? Our model would predict that firing rates during oscillatory episodes would increase compared to periods just prior to the episodes if the prior rates were low, and decrease if the prior rates were high. The transition would depend on the total input rate (Nf_i) to the neuron. Preliminary analysis of single neurons recorded in sensorimotor cortex of monkeys indicates that for units that were synchronized with LFP oscillations, firing rates during the oscillatory episodes increased for low prior rates and decreased for high prior rates, as predicted. This effect was not observed in neurons that were not synchronized with the LFP oscillations (Murthy and Fetz, unpublished observations).

In summary, for a simple biophysical model of the cortical neuron with three active conductances the spike rate could be increased significantly by increasing the synchrony among the inputs without necessarily altering the mean firing rates of the inputs. The range of parameters for which this effect is significant includes biologically plausible values ($Nwf_i < 9.4\ \mu S\ sec^{-1}$ or $0.5\ V\ sec^{-1}$). At higher firing rates synchrony in the inputs leads to a decrease in the average rates.

Acknowledgments

This work was supported by NIH Grants NS12542 and RR00166. V. N. Murthy was supported in part by a predoctoral fellowship from the W. M. Keck Foundation.

References

Abeles, M. 1982. Role of cortical neuron: Integrator or coincidence detector? *Isr. J. Med. Sci.* **18**, 83–92.

Abeles, M. 1991. *Corticonics: Neural Circuits of the Cerebral Cortex.* Cambridge University Press, Cambridge.

Bernander, Ö., Douglas, R. J., Martin, K. A. C., and Koch, C. 1991. Synaptic background activity influences spatiotemporal integration in single pyramidal cells. *Proc. Natl. Acad. Sci. U.S.A.* **88**, 11569–11573.

Bernander, Ö., Koch, C., and Usher, M. 1994. The effect of synchronous inputs at the single neuron level. *Neural Comp.* **6**, 622–641.

Bouyer, J. J., Montaron, M. F., and Rougeul, A. 1981. Fast fronto-parietal rhythms during combined focused attentive behavior and immobility in cat: Cortical and thalamic localizations. *Electroenceph. Clin. Neurophysiol.* **51**, 244–252.

Bush, P. C., and Sejnowski, T. J. 1993. Simulations of synaptic integration in neocortical pyramidal cells. In *Computation and Neural Systems*, F. H. Eeckman and J. M. Bower, eds., pp. 97–101. Kluwer Academic Publishers, Boston.

Chen, D.-F., and Fetz, E. E. 1993. Effect of synchronous neural activity on synaptic transmission in primate cortex. *Soc. Neurosci. Abstr.* **19**, 781 (319.7).

Eckhorn, R., Bauer, R., Jordan, W., Brosch, M., Kruse, W., Munk, M., and Reitböck, H. J. 1988. Coherent oscillations: A mechanism of feature linking in the visual cortex? *Biol. Cybern.* **60**, 121–130.

Engel, A., Kreiter, A. K., König, P., and Singer, W. 1991. Synchronization of oscillatory neuronal responses between striate and extrastriate visual cortical areas of the cat. *Proc. Natl. Acad. Sci. U.S.A.* **88**, 6048–6052.

Fetz, E. E., Toyama, K., and Smith, W. S. 1991. Synaptic interactions between cortical neurons. In *Cerebral Cortex*, A. Peters, ed., Vol. 9, pp. 1–47. Plenum Press, New York.

Freeman, W. J., and Van Dijk, B. W. 1987. Spatial patterns of visual cortical fast EEG during conditioned reflex in a rhesus monkey. *Brain Res.* **422**, 267–276.

Gray, C. M., and Singer, W. 1989. Stimulus-specific neuronal oscillations in the cat visual cortex. *Proc. Natl. Acad. Sci. U.S.A.* **86**, 1698–1702.

Hestrin, S. 1992. Activation and desensitization of glutamate-activated channels mediating fast excitatory synaptic currents in the visual cortex. *Neuron* **9**, 991–999.

Jagadeesh, B., Gray, C. M., and Ferster, D. 1992. Visually evoked oscillations of membrane potential in cells of cat visual cortex. *Science* **257**, 552–554.

Kenyon, G. T., Fetz, E. E., and Puff, R. D. 1990. Effect of firing synchrony on signal propagation in layered networks. In *Advances in Neural Information Processing Systems* **2**, D. Touretzky, ed., pp. 141–148. Morgan Kaufmann, San Mateo, CA.

Llinás, R., and Ribary, U. 1993. Coherent 40-Hz oscillation characterizes dream state in humans. *Proc. Natl. Acad. Sci. U.S.A.* **90**, 2078–2081.

Lytton, W. W., and Sejnowski, T. J. 1991. Simulations of cortical pyramidal neurons synchronized by inhibitory interneurons. *J. Neurophysiol.* **66**, 1059–1079.

Mason, A., Nicoll, A., and Stratford, K. 1991. Synaptic transmission between individual pyramidal neurons of the rat visual cortex *in vitro*. *J. Neurosci.* **11**, 72–84.

Murthy, V. N., and Fetz, E. E. 1992. Coherent 25-35 Hz oscillations in the sensorimotor cortex of awake behaving monkeys. *Proc. Natl. Acad. Sci. U.S.A.* **89**, 5670–5674.

Murthy, V. N., and Fetz, E. E. 1993. Effects of input synchrony on the response of a model neuron. In *Computation and Neural Systems*, F. H. Eeckman and J. M. Bower, eds., pp. 475–479. Kluwer Academic Publishers, Boston.

Nelson, J. I., Salin, P. A., Munk, M. H.-J., Arzi, M., and Bullier, J. 1992. Spatial and temporal coherence in cortico-cortical connections: A cross-correlation study in areas 17 and 18 in the cat. *Vis. Neurosci.* **9**, 21–37.

Reyes, A. D., and Fetz, E. E. 1993. Effects of transient depolarizing potentials on the firing rate of cat neocortical neurons. *J. Neurophysiol.* **69**, 1673–1683.

Sanes, J. N., and Donoghue, J. P. 1993. Oscillations in local field potentials of the primate motor cortex during voluntary movement. *Proc. Natl. Acad. Sci. U.S.A.* **90**, 4470–4474.

Softky, W. R., and Koch, C. 1992. The highly irregular firing of cortical cells is inconsistent with temporal integration of random EPSPs. *J. Neurosci.* **13**, 334–350.

Stafstrom, C. E., Schwindt, P. C., and Crill, W. E. 1984. Repetitive firing in layer V neurons from cat neocortex *in vitro*. *J. Neurophysiol.* **52**, 264–277.

Thomson, A. M., Girdlestone, D., and West, D. C. 1988. Voltage-dependent currents prolong single-axon postsynaptic potentials in layer III pyramidal neurons in rat neocortical slices. *J. Neurophysiol.* **60**, 1896–1907.

Wilson, M. A., and Bower, J. 1989. The simulation of large-scale neural networks. In *Methods in Neuronal Modeling: From Synapses to Networks*, C. Koch and I. Segev, eds., pp. 291–334. MIT Press, Cambridge, MA.

Received July 9, 1993; accepted January 24, 1994.